© NOV 2025 | IRE Journals | Volume 9 Issue 5 | ISSN: 2456-8880
DOI: https://doi.org/10.64388/IREV9I5-1712158

Response Surface Optimization of Quarry Pit Soil Washing and Fe Dissolution Kinetics

IDOKO JULIUS EMMANUEL[1], ABATYOUGH TERUNGWA MICHAEL[2], ABDULLAHI KASSIM[3]
[1,2] *Chemical sciences Department, Bingham University, Karu*

Abstract- ***Environmental pollution by quarry mining activities has proven to be harmful, mitigating these pollution levels by soil washing may not be effective for all pollution sites. Therefore, it is necessary to optimize these processes and identify the leaching mechanism. Quarry site soil sample was obtained from quarry pit. Physicochemical properties; specific gravity, particle size, porosity, elemental composition and pH were determined. The optimum leaching conditions were obtained following response surface methodology (RSM) approach using central composite design. Four (4) factors, particle size, time, agitation rate and solvent concentration were studied in twenty (20) experiments. Following optimization, the highest dissolution rate was observed to be 82 % with the reaction conditions of agitation rate (175 rpm), time (35 mins) and particle size (335 mm). The model's P-values were less than 0.05 while the correlation regression (R2) value of 0.7169 was obtained. The rate constants for the surface chemical reaction process (Ks) and the diffusion-controlled process (Kd) of Fe ranged from 0.007053-0.008023 min-1 for (Ks), and 0.730567-0.912173 min-1 for (Kd). The dissolution process was identified to be influenced by the diffusion-controlled mechanism having a rate constant value of > 0.9. The findings of this study will be helpful in mine reclamation and revision of soil washing protocol in the study area.***

Index Terms- ***Optimization, soil washing, iron, quarry, rate mechanism.***

I. INTRODUCTION

The presence of toxic metal ions in any environment is unacceptable due to their acute toxicity (Ali et al., 2020; Pruss-Ustun et al., 2016). There is growing apprehension about potential for exposure to Heavy Metals around the world. Quarrying involves mediation with the natural environment in complex and intricate ways which requires drilling, blasting, and the use of machinery to grade rock materials thereby exposing host communities to environmental and health hazards (Ayodele et al., 2014; Sonter et al., 2018; Akinluyi et al., 2019). The quarry mining operations cause leaching of heavy metals into groundwater, surface water, and further release into the ambient air which is capable of causing excessive exposure to heavy metals by residents of the quarry host communities (Ali et al., 2019). Hu et al. (2022) discovered that the ionization of acidic solutions causes an increase in free hydrogen ions, which corrodes the calcium and magnesium compounds in loess and further lowers the shear strength. It was discovered that a significant rise in hydrogen ion concentration results in a decrease in the diffuse double-layer thickness and alters the geotechnical characteristics of the soil including its compressibility and hydraulic conductivity (Zhou et al., 2024). mitigating these pollution levels by soil washing may not be effective for all pollution sites due to difficulties in understanding the mechanisms at play with varying environmental conditions, dissolution solutions and mineral pollutants in composition. Soil washing via solvent leaching is a heterogenous process and is determined by rate of diffusion transfer and rate of chemical reaction of dissolution therefore optimizing these processes will identify the most suitable conditions and the mechanisms of action by which the solvent is able to effectively carry out this washing activity (Hancock, 2021; Dhaliwal et al., 2020; Nguyen et al., 2021). The results will be helpful in mine reclamation and revision of soil washing protocol in the study area.

© NOV 2025 | IRE Journals | Volume 9 Issue 5 | ISSN: 2456-8880
DOI: https://doi.org/10.64388/IREV9I5-1712158

II. MATERIALS AND METHODS

2.1 Sample Collection and preparation

The quarry site soil was obtained from a community located in Nasarawa State Nigeria. The soil was crushed after which it was sieved and homogenized after oven drying it at 100 °C. Physicochemical properties like specific gravity, particle size, pH and porosity were determined. The sample was digested in 20ml of the (HNO_3-HCl 3; 1) aqua-regia on hotplate at 80 °C, after which the metal determination was done by using X-ray fluorescence (XRF).

2.2 Optimization of parameters for dissolution process

In order to optimize, simulate, and forecast the dissolution of metals in aqueous concentrations of the quarry site soil, the optimization of reaction conditions was investigated. This was optimized using a central composite design (CCD) design of experiment version 13.0. This was used to design the experiments and fit a quadratic response surface to experimental data, a total of twenty (20) experiments were carried out. The factors were chosen based on the leaching conditions that has proven to have the greatest impact from most studies. Analysis of variance (ANOVA) was used in statistical analysis.

2.3 The dissolution of metals from quarry site soil

The quarry site soil sample, 20 g at different particle sizes (45–600 µm) was added into the beaker containing 3.0 M HCl. The solution was mixed at varying agitation rates (90–490rpm). After the specified time, agitation rate, concentration and particle size, the samples were withdrawn from the beaker filtered and the liquid phase analyzed for metal content using the atomic absorption spectrophotometer (AAS). The dissolution rate of metal from quarry site soil was calculated following Seyed and Azizi (2018) and expressed in Equation 1.

$$R(\%) = \frac{CA\,X\,V}{CO\,X\,M} X\ 100 \qquad 1$$

From Equation 1, R (%) is the dissolution rate of Iron (conversion fraction), CA ($gL^{-}1$) is the concentration of iron in the dissolution liquor; V(L) is the dissolution liquor volume; Co is the metal content in the quarry site soil; and M (g) is the mass of the metal.

2.4 Kinetics of dissolution

The rate-limiting mechanism of the iron dissolution process was investigated using the surface chemical reaction (Equation 2) and the diffusion controlled (Equation 3) processes of the shrinking core model (Liddell, 2005; Hankook, 2021) The suitability of the shrinking core model emanates from the fact that it relates the conversion fraction (X) of the ore solid particle to the reaction rate constant (K) and reaction time.

$$1 - (1 - X)^{1/3} = K_s . t \qquad 2$$

$$1 - \frac{2}{3}X - (1 - X)^{\frac{2}{3}} = K_d . t \qquad 3$$

The rate constant for the surface chemical reaction (Ks) was obtained from the slope of the linear plot of 1 − (1 − X)1/3 versus time (t) using Equation 2. Also, the rate constant for the diffusion process (Kd) was obtained from the slope of the linear plot of 1 – 2/3 X – $(1 – X)^{2/3}$ versus time (t) using (Equation 3). The obtained rate constants with their corresponding R_2 values are used to determine the rate-limiting mechanism that influences the dissolution process of metals from ore.

III. RESULTS AND DISCUSSION

Table 1. Physicochemical properties

S/N	Property	Value
1.	Soil type	Sandy
2.	pH	6.4
3.	Particle size (µm)	750
4.	Porosity	38.00
5.	Specific gravity	2.614
6.	Fe (mg/l)	9.14
7.	Pb (mg/l)	2.03

3.1 Physicochemical properties

The physicochemical properties are shown in table 1. The soil type is sandy like, while the particle size was 750 µm and the porosity was 38.00, this composition would allow for free percolation of metals within soil matrices. The pH of the soil was slightly alkaline this is likely due to the location of the soil site been far from human and industrial activities. The specific

gravity was obtained as 2.614 been that of sandy soils. The elemental composition showed Fe and Pb among many other metals to have concentrations of 233.7 $mgkg^{-1}$. mining activity enhances heavy metal permeability in soil (Wang et al., 2023)

Table 2. Design of experiment

S/N	Agitation rate (rpm)	Time (min)	Particle size (um)	Fe Dissolution rate	Pb Dissolution rate
1	175	35	335	72	75
2	351.588	35	335	71	73
3	280	50	170	70	83
4	175	35	612.496	74	70
5	280	20	170	72	75
6	175	9.77311	335	72	76
7	175	35	335	71	73
8	-1.58825	35	335	70	72
9	70	50	500	62	74
10	175	60.2269	335	69	77
11	175	35	335	82	78
12	280	20	500	71	80
13	280	50	170	72	81
14	175	35	335	78	76
15	175	35	335	77	72
16	175	35	335	75	77
17	70	20	170	72	78
18	70	20	500	71	75
19	175	35	57.5042	67	70
20	70	50	170	70	73

3.2 Development and validation of RSM models for Predicting Dissolution rate

Table 2, shows the design of experiments for dissolution of Fe metal ions as a soil washing techniques. RSM was used in conjunction with CCD for the optimization. The Fe dissolution had the highest dissolution rate to be 82 % at the reaction conditions of agitation rate (175 rpm), time (35 mins) and particle size (335 mm). The magnitude of the correlation between the experimental and predicted values is established by the analysis of variance (ANOVA) as shown in Table 3. The prediction model equation is considered to be adequate when the F-value is high, while the significance of the prediction model is obtained when p-values are low. The model's P-values are observed to be less than 0.05 which indicates that the prediction models are significant. The model's generated F-values and p-values were 3.04 and 0.0437. The Model F-value of 3.04 implies the model is significant. There is only a 4.37% chance that an F-value this large could occur

due to noise. P-values less than 0.0500 indicate model terms are significant. The non-significant lack of fit observed is good since we want the model to fit.The correlation regression (R^2) for the variables indicates the degree of agreement between experimental results and theoretical predictions and was obtained as of 0.7169 in table 5. This suggests that the models are fit and good for analysis, The predicted and adjusted R^2 had a less than 0.2 difference as required. Adeq Precision measures the signal to noise ratio, a ratio greater than 4 is desirable as was obtained. Therefore, the model equation in equation 1, can be used to navigate the design space. The coefficient estimate represents the expected change in response per unit change in factor value when all remaining factors are held constant. When the factors are orthogonal the VIFs are 1; VIFs

© NOV 2025 | IRE Journals | Volume 9 Issue 5 | ISSN: 2456-8880
DOI: https://doi.org/10.64388/IREV9I5-1712158

greater than 1 indicate multi-collinearity, the higher the VIF the more severe the correlation of factors. As observed, all the VIFs were above 1 as seen in table 4.

Table 3. ANOVA for Fe Dissolution

Source	Sum of Squares	df	Mean Square	F-value	p-value	
Model	207.13	7	29.59	3.04	0.0437	significant
A-Agitation	9.99	1	9.99	1.03	0.3307	
B-Temp	21.27	1	21.27	2.19	0.1648	
C-Particle size	24.50	1	24.50	2.52	0.1384	
A^2	53.28	1	53.28	5.48	0.0373	
B^2	53.28	1	53.28	5.48	0.0373	
C^2	53.28	1	53.28	5.48	0.0373	
A^2C	42.50	1	42.50	4.37	0.0585	
Residual	116.67	12	9.72			
Lack of Fit	33.83	7	4.83	0.2917	0.9304	not significant
Pure Error	82.83	5	16.57			
Cor Total	323.80	19				

Final Equation in Terms of Coded Factor

Fe Dissolution rate = +75.84 +0.8554A -1.25B +2.08C +1.25AB +0.7500AC -1.00BC -1.92A^2 -1.92B^2 -1.92C^2 -3.58A^2C

Table 5. Fit Statistics

Std. Dev.		3.19	R^2	0.7169
Mean		71.90	Adjusted R^2	0.4024
C.V. %		4.44	Predicted R^2	0.3246
			Adeq Precision	5.2273

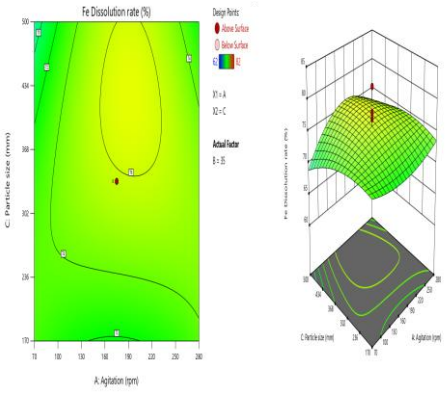

Figure 1 Contour and 3D plots for the interaction of agitation vs Time against Fe dissolution rate %

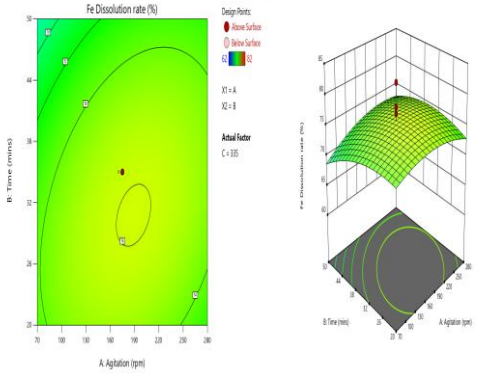

Figure 2 Contour and 3D plot for the interaction of agitation vs particle size against Fe dissolution rate %

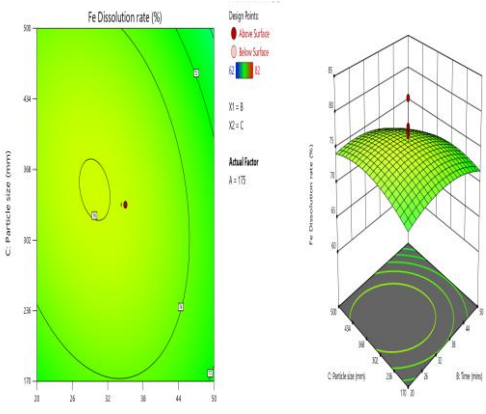

Figure 3 Contour and 3D plot for the interaction of Temp vs particle size against Fe dissolution rate %

© NOV 2025 | IRE Journals | Volume 9 Issue 5 | ISSN: 2456-8880
DOI: https://doi.org/10.64388/IREV9I5-1712158

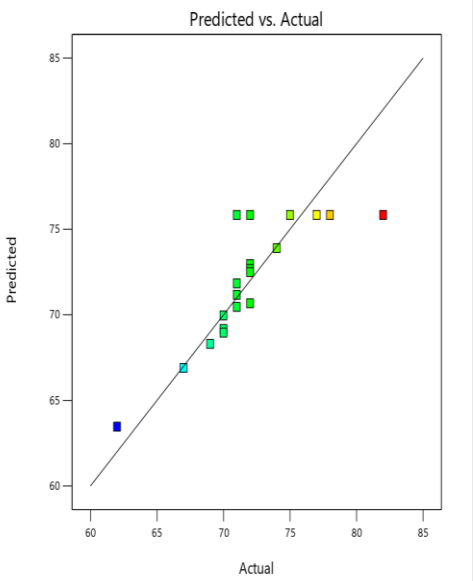

Figure 4. Plot of predicted vs actual Fe dissolution rates

3.3 Influence of operational parameters on responses for Fe dissolution

Contour plots were employed to explain the degree to which the operational factors interacted with their responses. As demonstrated in figures 1, 2 and 3. An elliptic contour denotes an interactive effect among parameters and a circular contour illustrates a non-interactive effect. The findings demonstrate that the elliptic contour plots for the optimization process observed in figure 2 effectively portray the interacting impacts of factors (reaction time, agitation rate and particle size) on the responses. While the circular plot of interactions in figure 1 and 3 were observed to have a non-interactive effect. The 3-D surface plots also denote the influence of parameter interactions on the dissolution rate of both Fe. The process of increasing or decreasing the values of parameters influences the rate of dissolution. As observed both the plot of particle size versus time and that of agitation rate versus time in figures 1 (b) and 3(b) respectively denotes that increasing both parameters attains optimization and results in subsequent reduction in dissolution rate, while the plot of particle size versus agitation in figure 2(b) suggests that increasing agitation rate will favour dissolution as opposed to increasing particle size. The plot of predicted versus actual experimental findings showed a good agreement in figure 4.

Table 6. Rate constants and R^2 at different agitation rates of Fe dissolution

	Surface Chemical process		Diffusion controlled process	
Agitation rates	KS	R^2	KD	R^2
50rpm	0.007053	0.96076	0.730567	0.95489
100 rpm	0.007604	0.96322	0.76355	0.97581
200 rpm	0.007734	0.97412	0.780217	0.98081
300 rpm	0.007881	0.9894	0.828557	0.98791
400 rpm	0.008023	0.98634	0.912173	0.9924

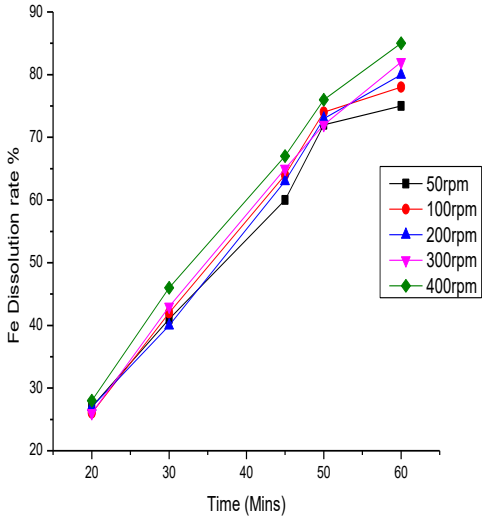

Figure 5. Effects of agitation rate (rpm) on the dissolution rate of Iron (Fe) from Karu quarry soil

3.4 Effect of agitation on iron (Fe) dissolution rate for quarry pit soil

The effects of agitation on the dissolution rates of iron were examined at room temperature in the ranges of 50–400 rpm and time in the range of 20-60 mins under the constant condition of 335-µm particle size. Results showed that the dissolution rates of iron increased rapidly at maximum time of 60 mins with an increase in agitation to the optimum Fe dissolution rates of 75.1% and 85.4 % at 300 rpm and 400 rpm,

respectively as shown in figure 5. The rate constants for the surface chemical reaction process (Ks) and the diffusion-controlled process (Kd) of Fe dissolution as shown in Table 6, are within the ranges of 0.007053-0.008023 min^{-1} for (Ks), and 0.730567-0.912173 min^{-1} for (Kd) respectively. From the rate constants, the rate-determining mechanism governing the dissolution of iron is shown to favourthe diffusion-controlled process. The R^2 values shown in Table 6 are also in support of the diffusion-controlled process as the rate determining mechanism. The experimental kinetic plots obtained at different agitation rates are shown in figures 6 (a,b).

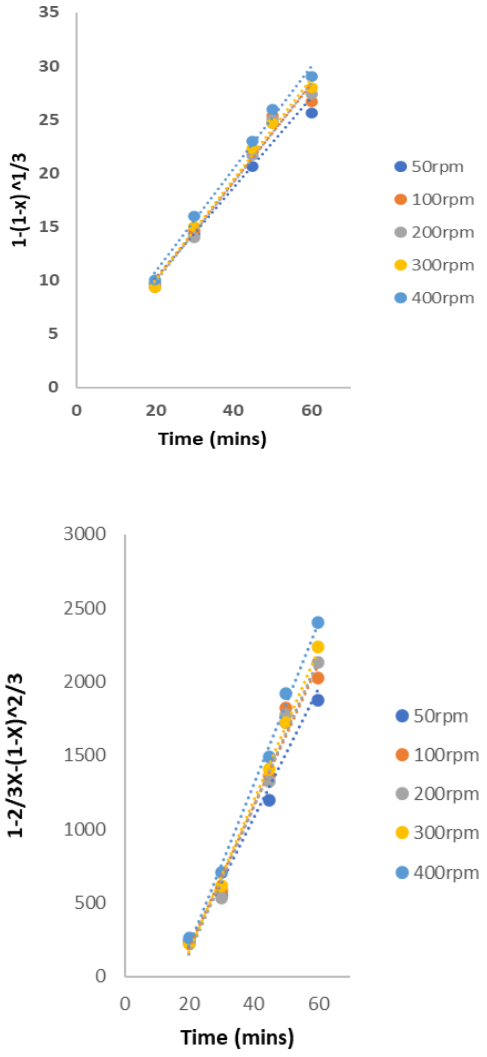

Figure 6. Plot of 1-(1-x)^1/3 and 1-2/3X-(1-X)^2/3 versus Fe dissolution time at different agitation rates.

IV. CONCLUSION

The study evaluates the dissolution process of iron as soil washing technique; the soil is characterized to be sandy and slightly acidic. The optimization process suggested agitation rate to be a good parameter to study the dissolution process, also following the rate constants, the dissolution process was identified to be influenced by the diffusion-controlled mechanism having a rate constant value of > 0.9 for the diffusion rate constant (Kd). Therefore, the dissolution process of Fe in the quarry pit soil involves the solubility of the dissolution solvent penetrating the core of the soil particles and not just its surface.

REFERENCES

[1] Ali H, Khan E & Ilahi I 2019. Environmental chemistry and ecotoxicology of hazardous heavy metals: Environmental persistence, toxicity, and bioaccumulation. Journal of Chemistry, 2019:14. https://doi.org/10.1155/2019/6730305

[2] Ali, I.; Hasan, M.A.; Alharbi, O.M.L. Toxic metal ions contamination in the groundwater, Kingdom of Saudi Arabia. J. Taibah Univ. Sci. 2020, 14, 1571–1579. [CrossRef]

[3] Dhaliwal, S. S., Singh, J., Taneja, P. K., & Mandal, A. (2020). Remediation techniques for removal of heavy metals from the soil contaminated through different sources: a review. Environmental Science and Pollution Research, 27(2), 1319-1333. https://doi.org/10.1007/s11356-019-06967-1.

[4] Hancock, G. R. (2021). A method for assessing the long-term integrity of tailings dams. *Science of the Total Environment*, *779*, 146083.

[5] Hu, W., Cheng, W. C., Wang, L., & Xue, Z. F. (2022). Micro-structural characteristics deterioration of intact loess under acid and saline solutions and resultant macro-mechanical properties. *Soil and Tillage Research*, *220*, 105382.

[6] Nguyen, T.H.; Won, S.; Ha, M.G.; Nguyen, D.D.; Kang, H.Y. Bioleaching for Environmental Remediation of Toxic Metals and Metalloids: A Review on Soils, Sediments,

and Mine Tailings. Chemosphere 2021, 282, 131108. [CrossRef] [PubMed]

[7] Pruss-Ustun A, Wolf J, Corvalan C, Bos R & Neira M 2016. Preventing disease through healthy environments: A global assessment of the environmental burden of disease from environmental risks. World Health Organization. https://apps.who.int/iris/handle/10665/204585

[8] Wang, C. C., Zhang, Q. C., Yan, C. A., Tang, G. Y., Zhang, M. Y., Ma, L. Q., ... & Xiang, P. (2023). Heavy metal (loid) s in agriculture soils, rice, and wheat across China: Status assessment and spatiotemporal analysis. *Science of The Total Environment*, *882*, 163361.

[9] Zhou, H., Yue, X., Chen, Y., & Liu, Y. (2024). Source-specific probabilistic contamination risk and health risk assessment of soil heavy metals in a typical ancient mining area. *Science of the Total Environment*, *906*, 167772.